Lab on a Chip

Devices and applications at the micro- and nanoscale

Accepted Manuscript

This article can be cited before page numbers have been issued, to do this please use: A. Jayaraman, D. Penarete-Acosta, M. Mittal, S. Chakraborty and A. Han, *Lab Chip*, 2025, DOI: 10.1039/D5LC00052A.

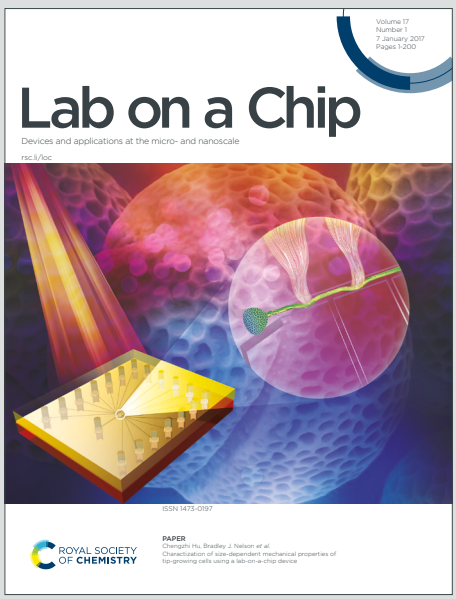

ROYAL SOCIETY OF CHEMISTRY

rsc.li/loc

View Article Online
DOI: 10.1039/D5LC00052A

Interplay Between Dietary Fiber, Macrophages and Colonocytes in a Microfluidic Model of Host-Microbiota Interactions in Colorectal Cancer

Daniel Penarete-Acosta[1,†], Mohet Mittal[2,†], Sanjukta Chakraborty[3], Arum Han[1,2,4], Arul Jayaraman[1,2*]

[1] Department of Biomedical Engineering, Texas A&M University
[2] Artie McFerrin Department of Chemical Engineering, Texas A&M University
[3] Department of Medical Physiology, College of Medicine, Texas A&M University
[4] Department of Electrical and Computer Engineering, Texas A&M University
* Corresponding author. arulj@tamu.edu
† Equal contribution.

Abstract

Dietary fiber has been consistently associated with a decreased risk of colorectal cancer development. While the apoptotic effect of dietary fiber microbial fermentation products such as short chain fatty acids on tumor colonocytes is well established, the role of these products on other components of the tumor microenvironment remains unexplored. Tumor associated macrophages play a critical role in tumor development in colorectal cancer; however, the effect of dietary fiber fermentation by microbiota on the interaction between macrophages and colonocytes in the colorectal cancer microenvironment has been difficult to dissect due to a lack of *in vitro* models of colorectal cancer containing immune cells, colonocytes, and microbiota. Recently, we developed a microfluidic model that facilitates the coculture of colorectal cancer spheroids with complex microbial communities. Here, we expand our model to include macrophages and employ it to study the impact of dietary fiber on macrophage-colonocyte interaction. We optimized monocyte differentiation parameters *in vitro* and demonstrated the capacity of our model to recapitulate changes in microbiota composition and metabolic output associated with dietary fiber administration *in vivo*. Coculture of colonocytes with microbiota and macrophages revealed that alterations in microbial production of short chain fatty acids derived from dietary fiber fermentation correlated with decreased colonocyte viability, possibly mediated by an increase in production of tumor

View Article Online
DOI: 10.1039/D5LC00052A

pro-apoptotic cytokines by macrophages. Our work highlights the capacity of microfluidic *in vitro* models to study the role of microbial metabolism of dietary molecules on colorectal cancer colonocyte viability in the presence of macrophages.

Introduction

Dietary fiber consumption has been extensively associated with lower risk of colorectal cancer (CRC) in humans(1). A causative link between consumption dietary fiber in the form of inulin and decreased incidence of aberrant crypt foci and tumor formation in mice has also been reported(2). Mechanistically, dietary fiber is metabolized by the colonic microbiota, which increases the abundance of fermentative bacteria and the production of short-chain fatty acids (SCFA) such as butyrate, propionate, and acetate(3–5). The capacity of these metabolites to induce apoptosis in colonocyte via mechanisms such as histone deacetylase inhibition is well established(6–11). For these reasons, prebiotic intervention with dietary fiber has been proposed as a preventive strategy against CRC(12).

The colorectal tumor microenvironment contains multiple types of immune cells that significantly impact tumor development and progression(13). Tumor-associated macrophages (TAMs) are abundant in carcinomas(14,15), where they exhibit either tumor supportive activity by favoring cancer cell proliferation(16,17) and migration(18–20), or tumor-suppressive activity by inducing tumor cell apoptosis via signals such as Tumor Necrosis Factor α (TNF-α)(21) and TRAIL(22). The activity of TAM is influenced by host-derived molecules present in the tumor microenvironment such as cytokines, chemokines, non-coding RNA, and oncoproteins(23,24).

In the colon, the microbiota and its metabolites have also been shown to modulate the activity of macrophages. Experiments in germ-free mice have shown that the microbiota regulates macrophage

View Article Online
DOI: 10.1039/D5LC00052A

recruitment and replenishment after the onset of inflammation, possibly via induction of chemokine production in colonocytes(25). Several pathogens associated with CRC, including *Fusobacterium nucleatum*, *Streptococcus gallolyticus*, and *Enterococcus faecalis*, promote a proinflammatory and immunosuppressive microenvironment by targeting macrophages(26). In terms of bacterial metabolites, lipopolysaccharide is a potent inducer of proinflammatory (M1-like) polarization in macrophages(27), while the SCFA butyrate promotes anti-inflammatory (M2-like) polarization in macrophages while boosting their phagocytic activity(28,29). Despite the high abundance of TAMs in tumors and the modulation of macrophage activity by microbiota, the effect of dietary fiber-induced changes in microbiota composition and function on TAM activity in CRC is not fully understood.

Intestinal and microfluidic models that facilitate the study of host-microbiota interactions, such as the gut-on-a-chip and HuMiX, have been successfully employed to gain insight into the effect of probiotics and prebiotics on epithelial physiology(30–32). However, the interplay among dietary molecules, microbiota and immune cells in the context of CRC remains unexplored. Previously, we developed a microfluidic device to study the interaction between HCT116 CRC colonocyte spheroids and murine colonic microbiota(33). Here, we expand the physiological relevance of this model by co-culturing a colonic microbial community with monocyte-derived macrophages with colonocytes in spheroids. We hypothesize that inulin fermentation by colonic microbiota impacts colonocyte viability in a macrophage-dependent manner. We use metabolomics, metagenomics, and protein and gene expression analysis to dissect the tripartite interaction between inulin, microbiota, and macrophages in our expanded CRC tumor microenvironment model. Our results contribute to our understanding of the effect of diet on host-microbiota interactions in the context of colorectal cancer and demonstrate the usefulness of physiologically relevant *in vitro* models to study these interactions.

View Article Online
DOI: 10.1039/D5LC00052A

Results

Inclusion of macrophages in an in vitro coculture model of CRC colonocyte-microbiota

To expand the physiological relevance of our previously developed colonocyte spheroid-microbiota coculture model(33), we incorporated macrophages derived from the monocyte cell line THP-1 into spheroids. It is well-established that *in vitro* differentiation of THP-1 cells with PMA results in a macrophage-like phenotype, but the PMA concentration and treatment time widely vary among studies and significantly impact differentiation success(34–36). Therefore, we first optimized PMA concentration and treatment time to maximize the development of macrophages and the expression of the macrophage surface marker Cluster of Differentiation 11b (CD11b). While THP-1 monocytes in culture are globular and remain in suspension, treatment of THP-1 cells with PMA resulted in cell attachment to the bottom of the culture plate with changes in both cell size and morphology (**Figure1A**). After PMA treatment for 24 h, the attached cells were circular in shape and displayed increased granularity under phase-contrast microscopy. As the treatment time increased beyond 48 h, cells became elongated at PMA concentrations greater than 50 ng/mL, while cells treated with lower concentrations remained globular and loosely attached. CD11b expression increased with treatment time and was maximum after 72 h of treatment with a PMA concentration of 50 ng/mL, as assessed by flow cytometry. Minimal differences in cell morphology were observed with higher PMA concentrations for the same duration of PMA stimulation (**Figure 1A**). Under these conditions, the mean fluorescence intensity in PMA-treated cells (indicative of Cd11b levels) increased 75% compared to untreated cells (**Figure 1B, C**). In addition, gene expression analysis revealed a significant upregulation in the transcription of genes related to monocyte differentiation and macrophage activity, including CD40, CD44, CD80, TNF-α, CD206, and CD163 (**Figure S1**). Therefore, treatment

View Article Online
DOI: 10.1039/D5LC00052A

with a PMA concentration of 50 ng/mL for 72 h was selected to induce THP-1 differentiation in all subsequent microfluidic device experiments.

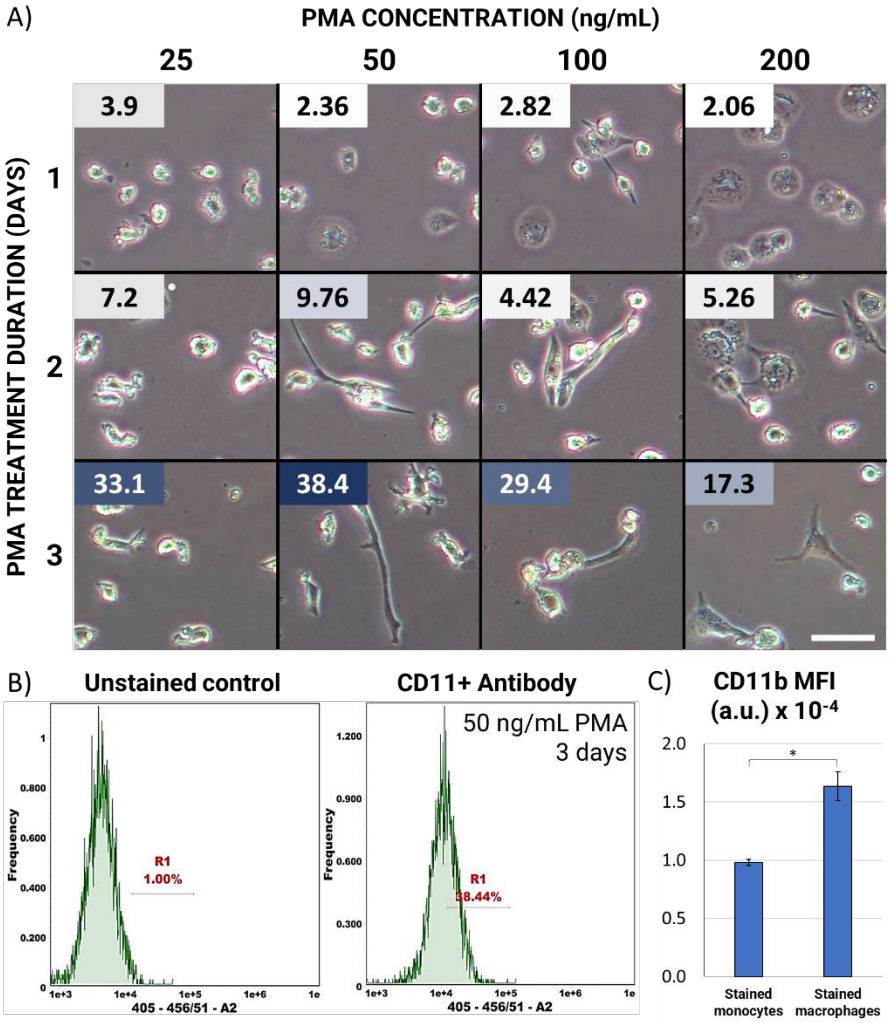

Figure 1 Optimization of PMA treatment for THP-1 monocyte differentiation.
A) Morphology of THP-1 cells after treatment with PMA in well plate. Boxed number indicates percentage of CD11b+ cells. Scale bar = 100 μm. B) Representative histograms of PMA-treated THP-1 cells stained with a fluorescently labelled CD11b antibody, and unstained control to account for background fluorescence. C) Mean Fluorescent Intensity (MFI) of stained THP-1 "monocytes" (untreated) and "macrophages" (PMA-treated, 50ng/mL for 3 days). * p-value < 0.05, n=3. Error bars represent SEM.

View Article Online
DOI: 10.1039/D5LC00052A

After optimizing THP-1 differentiation conditions, we cocultured HCT116 colonocytes and THP-1 cells in our previously developed model of colonocyte-microbiota interactions in colorectal cancer(33). In this model, colorectal cancer spheroids and colonic microbiota are cultured in separate, continuously perfused compartments and exchange secreted metabolites through a porous membrane (**Figure 2A-C**). To include macrophages in this model, a 1:1 suspension of THP-1 monocytes and HCT116 colonocytes in Matrigel was injected in the mammalian cell culture chamber on day 0 and perfused with media containing the optimized PMA concentration for 3 days to foster monocyte polarization during colonocyte spheroid formation before coculture with microbiota and/or treatment with inulin (**Figure 2D)**. Treatment with PMA during co-culture with HCT116 cells resulted in a significant increase in the expression of CD11b in THP-1 cells, with 60% of cells becoming positive and a 2.5-fold increase in MFI compared to untreated THP-1 monocytes in flask cultures (**Figure 2E, F**). To better understand the contribution of different factors to CD11b overexpression, we exposed Matrigel-embedded THP-1 cells to HCT116 in co-culture, PMA treatment, or combinatorial treatment, using transwell inserts (**Figure S2A**). Gene expression analysis revealed that both HCT116 alone and PMA alone increased the transcription of CD11b in THP-1 cells, while combinatorial treatment resulted in the highest expression levels (Figure S2B). These results confirmed the differentiation of THP-1 cells into a macrophage-like phenotype in the microfluidic coculture model.

View Article Online
DOI: 10.1039/D5LC00052A

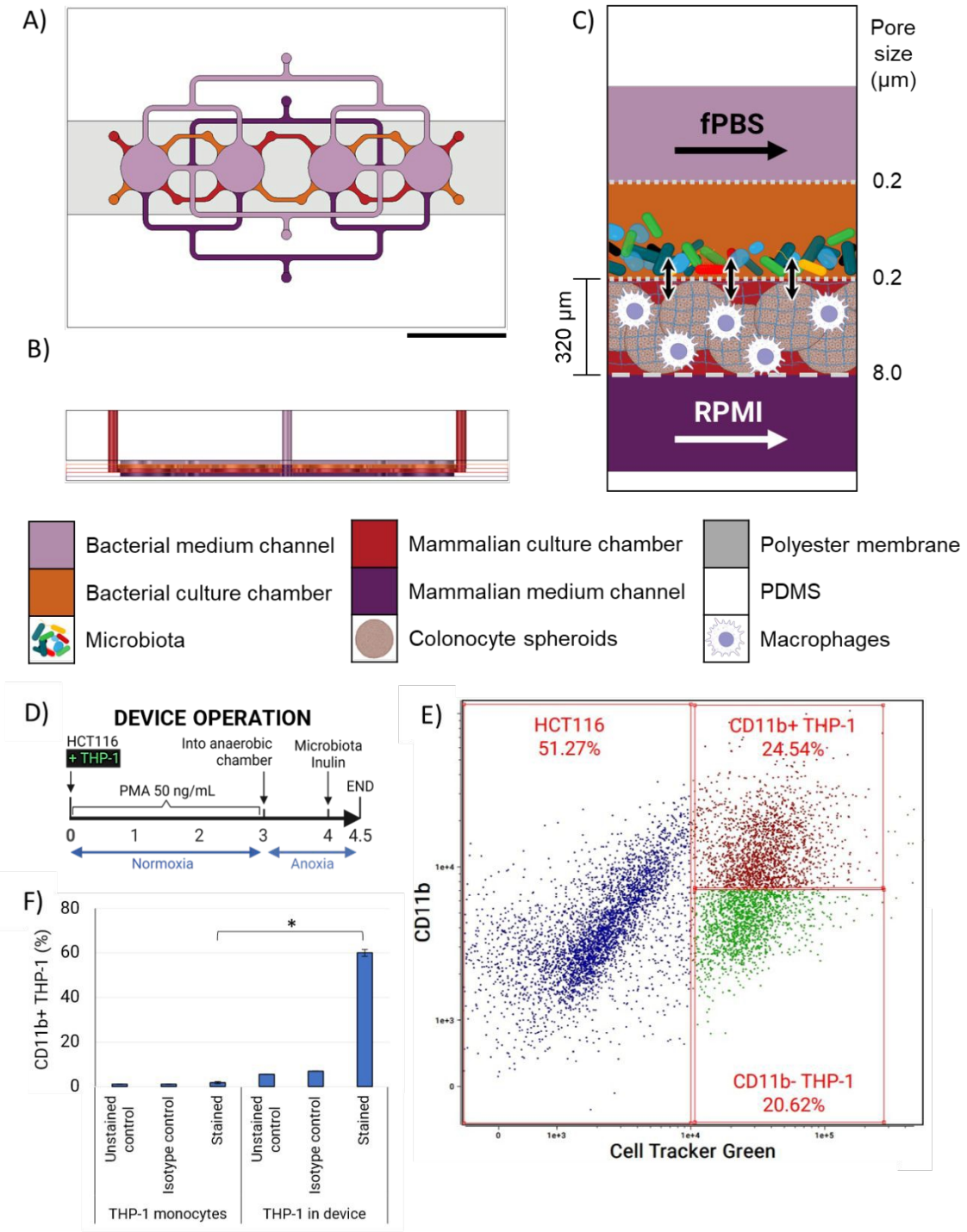

Figure 2 Microfluidic device design and operation.

A) Top and B) cross-sectional views highlighting media channels and culture chambers. Scale bar = 1 cm. C) Schematic representation of device cocultures. Confined bacterial, colonocyte and macrophage populations interact via small molecules during perfusion of fecal PBS (fPBS) through the top channel and growth media (RPMI) through the bottom channel. D) Experimental schedule of device coculture. E) Dot-plot of HCT116 – THP-1 cells after device coculture. THP-1 cells were loaded with CellTracker

View Article Online
DOI: 10.1039/D5LC00052A

Green dye prior to coculture. The CD11b positivity threshold was defined based on unstained control. F) Percentage of CD11b+ THP-1 monocytes (control) and THP-1 cells after treatment with PMA during device coculture. * p-value < 0.05, n=3. Error bars represent SEM.

Inulin induces changes in microbiota abundance and function

To validate the use of our model to study the impact of dietary fiber on microbiota, we characterized the effect of inulin treatment on SCFA production and alterations in microbiota composition. The levels of three SCFAs (acetate, propionate, and butyrate) produced by anaerobic microbiota co-cultured with HCT116 cells after inulin treatment were analyzed using GC-MS. Treatment with inulin for 12 h resulted in a 95% (from 234 μM to 12 μM) decrease in acetate and a less pronounced decrease of 44% (from 12 μM to 7 μM) in butyrate levels, relative to the untreated controls. On the other hand, a 25% increase (from 50 μM to 63 μM) in propionate levels was observed (**Figure 3A**), indicating differential effect of inulin exposure on the production of SCFAs by the microbial community. Inulin treatment also induced bacterial proliferation, as noticed by a 21% increase in the optical density of the culture at 600 nm (**Figure 3B**).

Metagenomic (16S rRNA) analysis of the microbiota community after inulin treatment revealed minimal taxonomic changes in the composition upon treatment with inulin. Regardless of inulin treatment, the microbiota cultured on chip was dominated by members of the *Bacteroides* genus (70%), and 24 other genera commonly associated with gastrointestinal tract microbiota, such as *Blautia*, *Ruminococcus*, and *Akkermansia*, that were present at a relative abundance higher than 1% (**Figure 3C**). The β-diversity analysis shows that while inulin treatment resulted in a significant change in overall microbiota composition, there was an overlap between ellipses that define a 95% confidence interval around the centroid of each treatment (**Figure 3D**). This result is consistent with the small but significant change in the abundance of members of the community upon treatment with inulin, including *Akkermansia* (0.45-

View Article Online
DOI: 10.1039/D5LC00052A

fold), *Dysgonomonas* (0.88-fold), *Oscillospira* (0.87-fold), *Anaerostipes* (1.96-fold), and *Lactobacillus* (1.62-fold) (**Figure 3E**), as well as a 1.2-fold increase in the relative abundance of 6 genera (*Pseudobutyrivibrio, Anaerotruncus, Anaerobranca, Erysipelothrix, Turicibacter, Lachnospira, Peptoniphilus*) that did not reach statistical significance. The largest effect of inulin on microbiota composition was a 4% increase in the abundance of the genus *Bacteroidetes*, while the largest change in relative composition was a 1.96-fold increase in the abundance of the genus *Anaerostipes*.

View Article Online
DOI: 10.1039/D5LC00052A

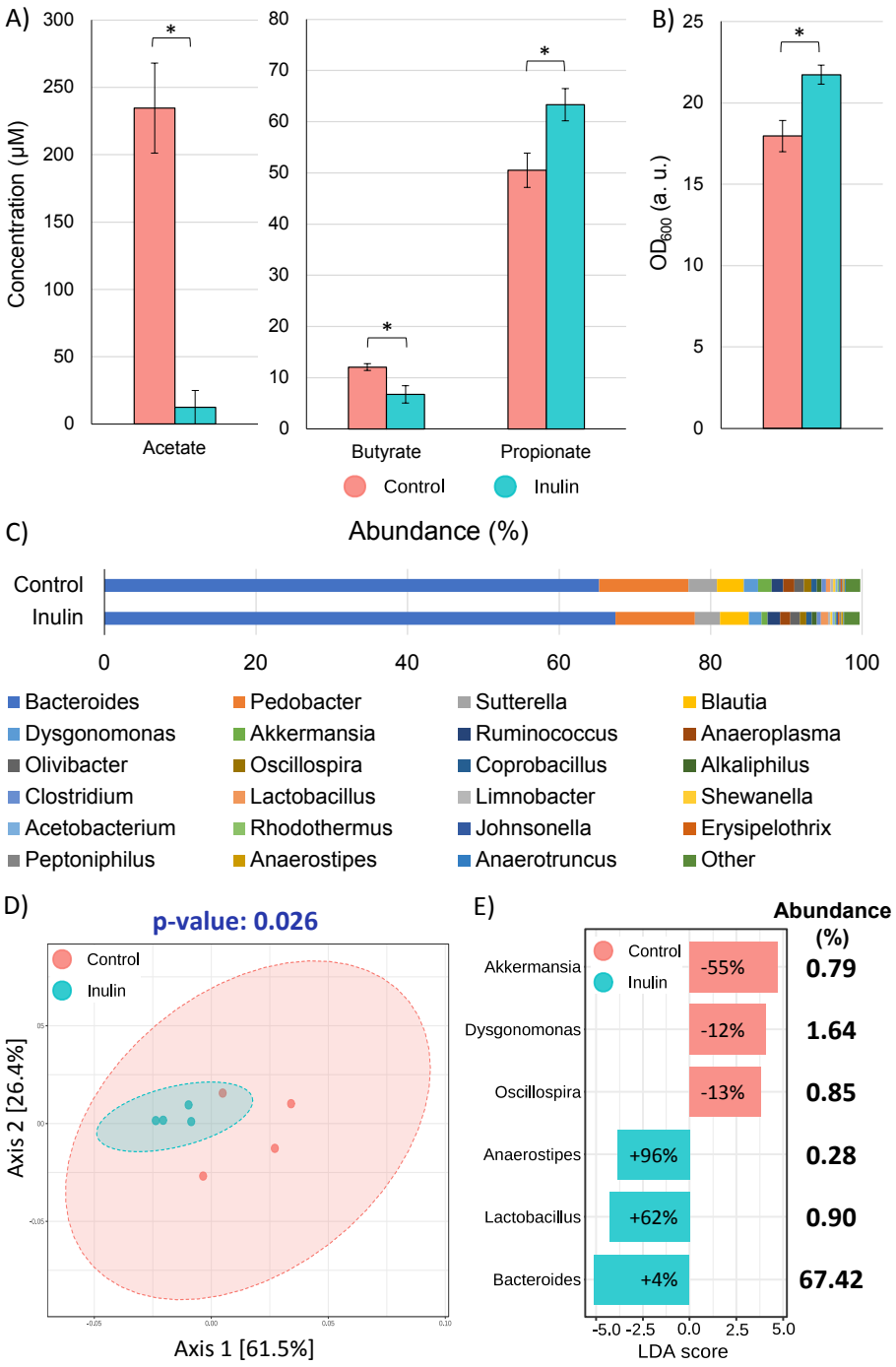

Figure 3 Effect of inulin on microbiota function, abundance, and composition.
A) SCFA concentration in the bacterial culture chamber upon treatment with fPBS supplemented with 2.5% (w/v) inulin. B) Optical density of microbiota extracted from the device after inulin treatment. * p-value < 0.05, n=3. C) Microbiota composition at the genus level, D) β-diversity analysis, and E) LEfSe comparison of microbiota after treatment with inulin (2.5% w/v in fPBS) or control (fPBS) on chip. Percentages in the bars in E) correspond to relative change in the abundance of a genera normalized to abundance in control, and Abundance (%) corresponds to the composition in the inulin-treated microbiota.

View Article Online
DOI: 10.1039/D5LC00052A

Inulin enhances macrophage-mediated decrease in colonocyte viability in a microbiota-dependent manner

To evaluate the impact of inulin on macrophage-microbiota-colonocyte interactions, we cocultured HCT116 colonocytes with THP-1 macrophages and microbiota for 12 hours (**Figure 4A**). HCT116 spheroids without THP-1 macrophages, HCT116 spheroids and microbiota without THP-1 macrophages, and HCT-116, THP-1, and microbiota without inulin were used as controls to assess the impact of each component on HCT116 cell viability. After device coculture and treatment, cells were extracted from device and disaggregated into a single cell suspension. The viability of each cell type was assessed employing a combination of CellTracker Green dye for labelling THP-1 cells and PI staining for labelling dead cells (**Figure 4B**). Inulin treatment of microbiota in coculture with HCT116 colonocytes and THP-1 macrophages resulted in a decrease of 17% in colonocyte viability relative to control treatments without macrophages, microbiota, or inulin (**Figure 4C**). In contrast, THP-1 viability remained relatively unchanged, regardless of the presence of microbiota or treatment with inulin (**Figure 4D**). The reduction in colonocyte viability correlated with a 4-fold increase in *TNF-α* transcription with respect to cocultures without either microbiota or inulin (**Figure 4E**), suggesting an effect of inulin metabolism by the microbiota on pro-inflammatory cytokine production and macrophage-colonocyte interaction.

View Article Online
DOI: 10.1039/D5LC00052A

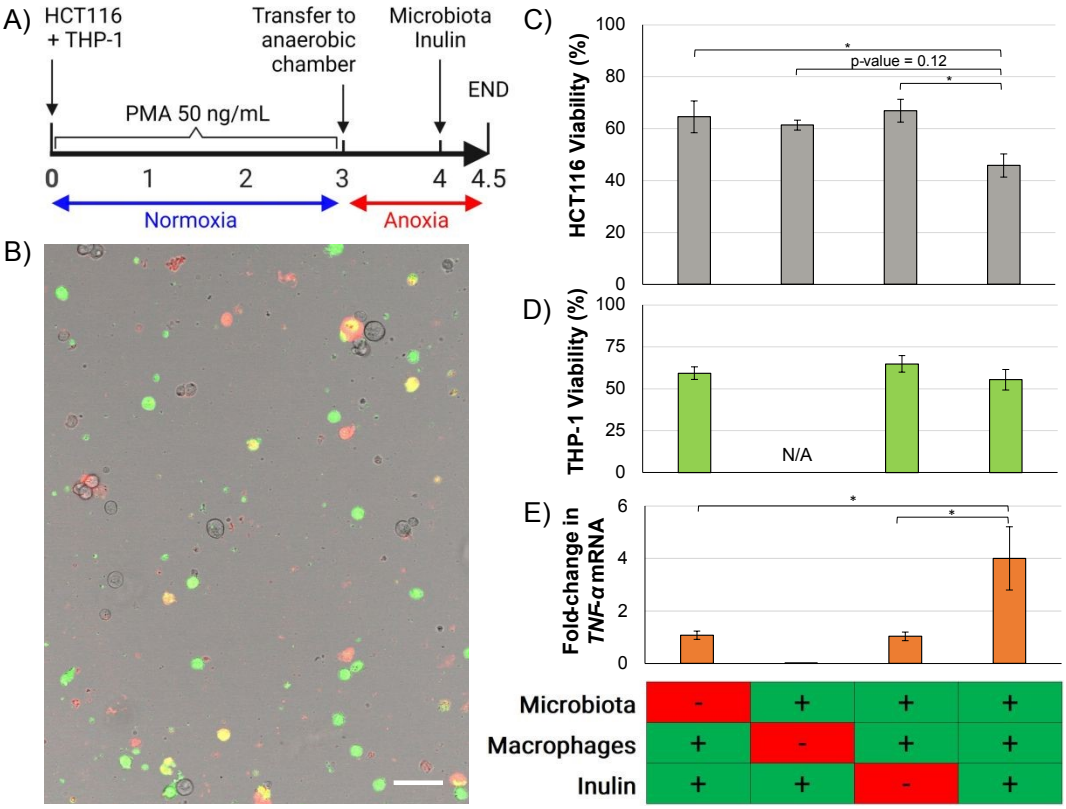

Figure 4 Effect of macrophages, inulin, and microbiota on colonocyte viability.
A) Experimental schedule. B) Representative image of multicolor strategy to distinguish viability by cell type after extraction of cells from microfluidic device. Unstained: viable HCT116 cells. Red: dead HCT116 cells. Green: viable THP-1 cells. Yellow: dead THP-1 cells (Green + Red). Scale bar = 50 µm. C) HCT116 and D) THP-1 viability upon combinatorial treatment with microbiota and inulin. E) Associated fold-change in *TNF-α* transcription in device co-cultures. * p-value < 0.05, n=3. Error bars represent SEM.

Inulin-derived SCFAs increase the concentration of pro-inflammatory cytokines during THP-1- HCT116 co-culture

To gain deeper understanding of the mechanisms through which microbial fermentation of inulin might increase macrophage toxicity against cancer cells, HCT116 and THP-1 cells transwell co-cultures were treated with prepared SCFA mixtures matching the SCFA concentrations measured from inulin-treated devices co-cultures ("inulin-derived SCFA"), control devices without inulin ("inulin-negative") , and

View Article Online
DOI: 10.1039/D5LC00052A

monoculture controls, following the same experimental schedule as device co-cultures (**Figure 5A**). Quantification of culture supernatants for pro-inflammatory cytokines revealed a significant upregulation of IL-1β, IFN-γ, TNF-α, MCP-1, IL-8, IL-12p70 and IL23 after treatment of co-cultures with inulin-derived SCFA mixture, compared to control (**Figure 5B**). In addition, the cytokine IL-33, which was undetectable in control co-cultures, also followed this trend; however, since the levels were below the limit of detection in control cultures, it was not possible to assign statistical significance. Individual treatment of each cell type with the SCFA mixtures suggested HCT116 as the cell type likely responsible for the increased production of MCP-1, IL-23, TNF-α and IL-33, while THP-1 was identified as the likely producer of IL-1β and IL12p70 (**Figure 5B**). Interestingly, co-culture of THP-1 macrophages with HCT116 cells significantly reduced the concentration of the aforementioned cytokines, and treatment with inulin-derived SCFA mixture partially recovered pro-inflammatory cytokine levels.

View Article Online
DOI: 10.1039/D5LC00052A

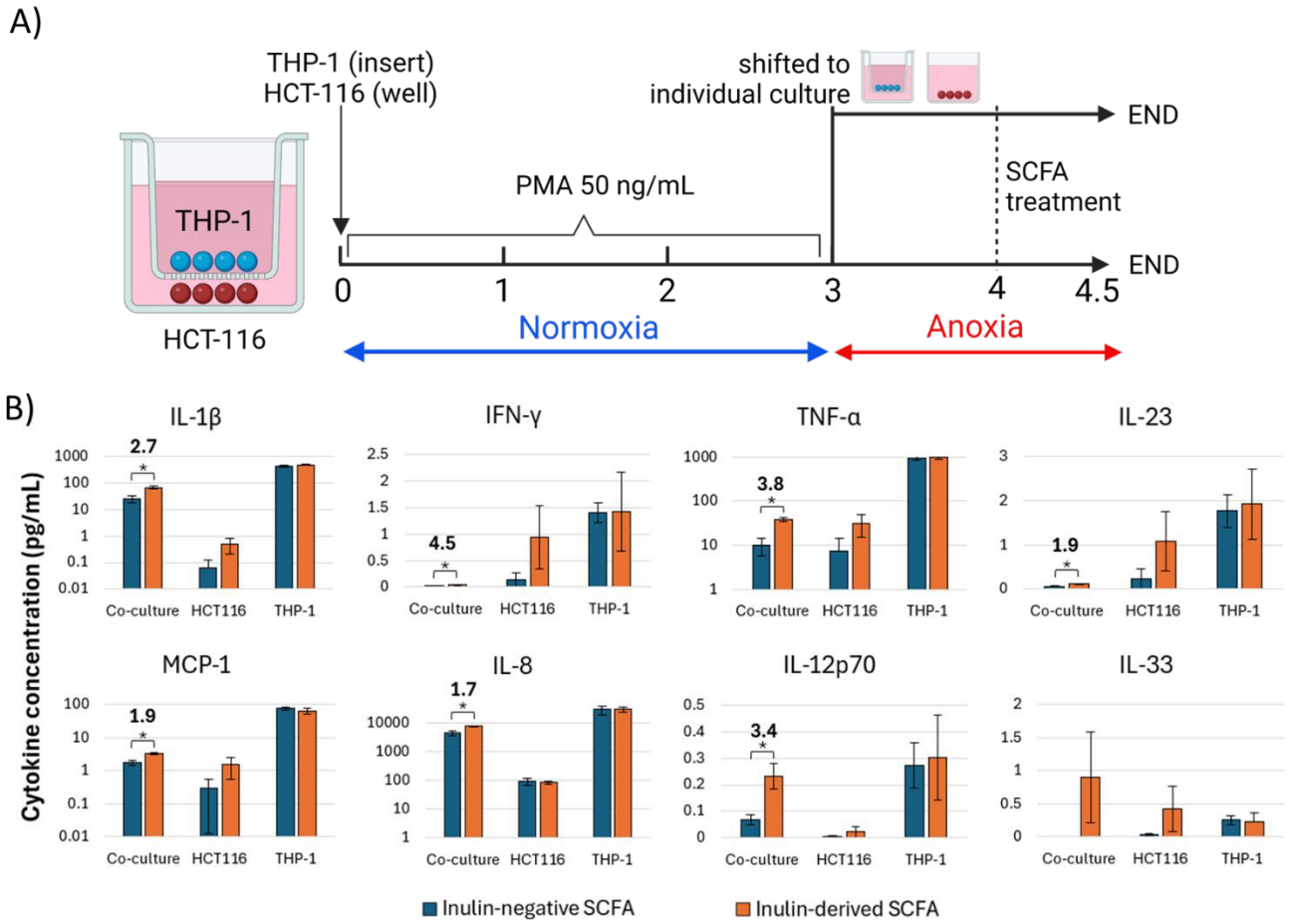

Figure 5 Effect of Inulin-derived SCFA mixture on pro-inflammatory cytokine levels.
A) Experimental design of co-culture and mono-culture treatment with SCFA mixtures. B) Quantified pro-inflammatory cytokine concentrations. Bold number above bars indicate fold change in cytokine concentration, normalized to "Inulin-negative SCFA". * p-value < 0.05, n=3. Error bars represent SEM.

Discussion

Dietary fiber intake significantly correlates with decreased incidence of CRC prospective human cohort studies(1,37). Administration of inulin to murine CRC models has been shown to result in altered microbial abundance, changes in microbiota composition, and modulation of SCFA production(2,38). In our model, inulin treatment significantly increased microbial proliferation and abundance (**Figure 3B**), which agrees with the reported increased in cecal weight in mice and rats that has been partly attributed to increased bacterial abundance(39,40). Inulin treatment also statistically altered the overall composition of the microbiota, although the impact on the abundance of most genera was not significant (**Figure 3C-**

View Article Online
DOI: 10.1039/D5LC00052A

D). Members from the genus *Bacteroides*, an abundant member of human and murine intestinal microbiota that outcompetes other inulin fermenters such as Bifidobacteria *in vitro*(41), were detected in the microbiota cultured in our model and increased in abundance with inulin treatment. Therefore, the small impact of inulin on the overall microbiota composition could be a consequence of interspecies competition dominated by *Bacteroidetes* (**Figure 3E**). The abundance of the genera *Lactobacillus* and *Anaerostipes*, reported to increase in individuals upon ingestion of inulin(42–45), also significantly increased in our model.

Inulin treatment resulted in a significant increase in propionate (**Figure 3A**), which is the most consistently reported effect of inulin administration in murine models(46–51). The increase in propionate concentration also agrees with the high abundance of *Bacteroides* in the community, as members of this genus ferment inulin into propionate(52,53). The effect of inulin administration on the levels of acetate in the colon *in vivo* have been inconsistent, with at least two studies showing either no effect or a decrease in abundance(46,48). In our model, inulin treatment resulted in a significant decrease in extracellular acetate, which might have been caused by the conversion of acetate into acetyl-CoA for fatty acid biosynthesis and TCA cycle intermediates under low oxygen conditions to support proliferation(54). While inulin consumption is frequently associated with increased butyrate levels in mice and rats(47–49,51), a decrease in butyrate was observed in our model. Crucially, inulin and fructose fermenters are known to produce acetate that is then employed by other species to produce butyrate(55); therefore, the lack of an increase in butyrate could simply be a consequence of the short treatment time (12 hours) compared to weeks of inulin feeding in *in vivo* experiments(46–51). It is also important to highlight that the response of gastrointestinal microbiota to dietary fiber interventions *in vivo* is heavily dependent on initial microbiota composition, which has resulted in significant inter-subject and inter-study

View Article Online
DOI: 10.1039/D5LC00052A

variability(56–59) and may explain the differences between some our results and other studies. Overall, our model recapitulated the increase in microbiota abundance and changes in SCFA production induced by inulin *in vivo*, which supports its use to study the effect of this dietary fiber on colonic microbiota *in vitro*.

Based on the immunomodulatory activity of the microbiota in the colon and the pivotal role of macrophages in CRC, we hypothesized that the changes in microbiota induced by inulin impact macrophage-colonocyte interaction in our coculture model. Our results show a macrophage-dependent decrease in colonocyte viability upon coculture with microbiota treated with inulin (**Figure 4C**). This correlated with an increase in the transcription and secretion of TNF-α in the co-cultures(**Figure 4E, Figure 5B**), a proinflammatory cytokine that triggers apoptosis and necrosis in tumor-derived cell lines(21), including CRC cell lines(60,61). The increase in TNF-α production correlated with a decrease in acetate and an increase in propionate with inulin-treated device co-cultures (**Figure 3A**), which agrees with the reported strong inhibition of TNF-α production by acetate(62).Treatment of THP-1 and HCT116 colonocyte transwell co-cultures with a mixture of SCFA matching the concentrations from inulin-exposed device cocultures confirmed an increase in the abundance of proinflammatory cytokines (**Figure 5B**) that have been reported to promote macrophage recruitment and activation (MCP-1, IL-8)(63,64), phagocytic activity (IL-23)(65,66), and tumor cell apoptotic induction by macrophages (IL-12p70, IFN-γ)(67–69). While these observations might explain the macrophage-dependent decrease in colonocyte viability upon treatment with inulin, the mechanisms associated with the possible role of these cytokines in this context require further study.

Importantly, cytokines such as IL-23 and IL-8 can also induce cancer cell proliferation(70,71) in a matter that might be dependent on the action of multiple immune cells in the tumor microenvironment(13); therefore, increased model complexity by incorporating additional immune cell

View Article Online
DOI: 10.1039/D5LC00052A

types such as T- cells will likely improve the physiological relevance and elucidation of underlying mechanisms. Inulin-induced changes in the abundance of other microbial metabolites that affect pro-inflammatory cytokine production in macrophages, such as lipopolysaccharide and indole derivatives(72), may also explain the observed effect of inulin on colonocyte viability, and require further characterization.

A strong association between dietary fiber consumption and lower CRC incidence has been reported by metanalyses of prospective cohort studies(1,37). The preventive activity of dietary fiber against colorectal cancer has been attributed to the increased production of total SCFA by microbiota and its direct proapoptotic effect on colonocytes(73,74). Importantly, a large number of dietary intervention studies in humans have found little to no effect of inulin ingestion on fecal SCFA concentration(75–80). Our results suggest that dietary fiber may reduce cancer colonocyte viability via proinflammatory cytokine production in macrophage and cancer cell co-cultures, even in the context of a decreased total abundance of SCFA. The microbiota-mediated immunomodulatory activity by inulin proposed here is conceptually similar to the improved Natural Killer cell cytotoxicity in a rat model of CRC upon inulin administration (81), as well as the reduction in xenograft tumor growth in mice upon inulin administration via microbiota-dependent T-cell activation(82). Since both diet and immune cell activity are key factors in CRC, the mechanisms underlying the potential immunomodulatory effect of dietary fiber on the immune component of the tumor microenvironment require further study.

The role of macrophages in CRC is controversial(83,84). While *in vitro* studies have shown that macrophages induce CRC colonocyte proliferation and migration(16–20), epidemiological studies show that high macrophage infiltration in CRC tumors is often associated with better prognosis(85). Importantly, *in vitro* studies have failed to consider the hypoxic, ECM-rich, three-dimensional microenvironment of tumor tissue(13), as well as the impact of the microbiota and its products on

View Article Online
DOI: 10.1039/D5LC00052A

macrophage activity. Our results using a physiologically-relevant microenvironment that contains both microbiota and dietary molecules show a macrophage-dependent decrease in colonocyte viability *in vitro*, more consistent with epidemiological data. We also identified an increase in the abundance of inflammatory cytokines upon inulin-derived SCFA treatment in a complex macrophage-cancer cell co-culture, while treatment of monocultures failed to capture these effects. These observations support the potential of complex *in vitro* systems and microfluidic technology to study complex host-microbiota interactions *in vitro* in a manner that is more relevant than conventional cell culture experiments(86).

Future endeavors on model development and biological characterization are poised to increase the impact of our findings. Current co-cultures with microbiota last for 12 hours, which is sufficient to observe significant changes at the transcription and translation levels. However, extended fermentation times of up to 24 hours might be required to ensure complete inulin consumption and more significant changes in microbiota composition(87,88). While the changes in microbiota composition upon inulin treatment we observed are consistent with reported effects of inulin *in vivo*, a more extended coculture time might be required to observe more pronounced changes in composition which would better recapitulate the shifts in composition observed *in vivo.* The mechanisms of inulin-microbiota-macrophage interaction proposed here are based on correlation among variables and therefore require further investigation to demonstrate causality. This could be accomplished by employing selective inhibitors (e.g., against TNF activity)(89), using synthetic or controlled microbial communities(59), and macrophages with diminished TNF-α production capacity(90). Further characterization of the microbiota via metabolomics, as well as macrophages via RNA sequencing and expanded immunotyping, would be useful to identify correlations between microbial metabolism, macrophage activation, and colonocyte viability. The use of more relevant sources of macrophages, such as bone-marrow derived monocytes, would also increase the biological

View Article Online
DOI: 10.1039/D5LC00052A

relevance of future studies(91). Finally, a diverse group of dietary fibers may increase our understanding of the dynamics of dietary fiber fermentation and changes in microbiota and macrophage activity.

Methods

Mammalian cell culture and reagents

The human colorectal cancer cell line HCT116 (CCL-247) was obtained from ATCC and cultured in RPMI 1640 medium (Corning) supplemented with 10% FBS (Atlanta Biologicals), GlutaMAX, HEPES, and NEAA (Gibco). The human monocyte cell line THP-1 was obtained from ATCC and cultured in RPMI 1640 medium (Corning) supplemented with 10% FBS (Atlanta Biologicals), 1% GlutaMAX, 1% HEPES, 1% NEAA (Gibco), and 2-mercaptoethanol (Sigma-Aldrich) to a final concentration of 0.05 mM. THP-1 cultures were maintained at a density between $2x10^5$ and $9x10^5$ cells/mL. For device coculture experiments, THP-1 cells were labelled with 2 μM CellTracker Green CMFDA (ThermoFischer Scientific) in serum-free media for 45 minutes.

Optimization of THP-1 differentiation

THP-1 monocytes were differentiated to macrophages with phorbol 12-myristate 13-acetate (PMA, Sigma-Aldrich). THP-1 differentiation was optimized using ~$5x10^5$ cells/mL in a 1 mL culture tube and treated with PMA to a final concentration of 25, 50, 100 or 200 ng/mL. Cells were incubated at 37°C for 1, 2, or 3 days. To detach PMA-treated THP-1 cells from culture tubes for flow cytometry analysis, the PMA-containing media was replaced with PBS with 10 mM EDTA, incubated on ice for 15 minutes, and detached by repeated pipetting.

Microfluidic device construction and operation

View Article Online
DOI: 10.1039/D5LC00052A

Device construction and operation was performed as previously described(33). The device consists of four PDMS layers separated by three porous polyester membranes (**Figure 2A-C**). Thin patterned PDMS layers were obtained by pouring uncured PDMS mix (Sylgard 184®) on a 3D-printed patterned mold (Stratasys, Inc.) with a total height of 500 μm and a pattern height of 160 μm, and then the PDMS was cured for 1 hour at 70 °C. Biopsy punches were used to create culture chambers (D = 5 mm, final chamber volume of ~10 μL) and open access to the perfusion channels and culture chambers (D = 1 mm). The device was assembled layer-by-layer using a thin layer of uncured PDMS as glue, and a polyester membrane was sandwiched between each pair of layers. The device was connected to media reservoirs by flexible 23-Gauge Tygon® medical tubing (Saint Gobain) using 20-Gauge stainless steel connectors detached from dispensing needles (Jensen Tools). To minimize the formation of bubbles during operation, the assembled device was placed underwater and vacuumed to a final pressure of $3x10^{-2}$ mbar for 24 hours; then, the device was autoclaved (121 C, 16 PSIG, 45 minutes) and kept covered in sterile water during operation. This protocol sterilized the device and prevented bubble formation. The device was held underwater for the duration of the experiment and only brought out of water for cell injection.

For colonocyte injection, the mammalian culture chambers in the device were seeded with 50% v/v Matrigel diluted in RPMI medium containing either ~$4x10^6$ HCT116 cells/mL or ~$2x10^6$ HCT116 and ~$2x10^6$ labelled THP-1 cells/mL. After cell seeding, devices were perfused with antibiotic-free RPMI through the mammalian medium channel, while PBS supplemented with 50 ng/mL of PMA was perfused through the bacterial chamber. On day 4 of culture, the bacterial chamber media was replaced with PMA-free PBS, and devices were transferred and operated in an anaerobic chamber for 24 hours. On day 5, murine fecal microbiota was obtained from freshly-voided fecal pellets obtained from 8 to 12 weeks-old wild-type C57BL/6 female mice fed a standard chow diet and processed as previously described to isolate

View Article Online
DOI: 10.1039/D5LC00052A

microbiota and prepare fecal PBS (fPBS)(33). The fecal slurry containing microbiota was introduced into the bacterial chamber, and the PBS in the bacterial medium reservoir was replaced with sterile-filtered fPBS or fPBS supplemented with inulin at a concentration of 2.5% (w/v) (Spectrum Chemical). Cocultures proceeded for 12 hours.

For sample collection, the microbiota in the bacterial culture chamber was collected by pipetting, to a final volume of ~10 µL per chamber. Bacteria were pelleted by centrifugation at 10000g for 10 minutes. The supernatant was used for SCFA analysis by GC-MS while the bacterial pellet was resuspended in 500 µL of PBS, the OD_{600} noted, and centrifuged (10000g, 10 minutes) to obtain a bacterial cell pellet. All pellets were stored at -80 °C until further processing. Next, the mammalian hydrogels were recovered by carefully disassembling the device with a scalpel. For flow cytometry and viability analysis, the mammalian hydrogels were placed on ice in PBS with 10 mM EDTA for 15 minutes and disaggregated by repeated pipetting to obtain single cell suspensions. For gene expression analysis, hydrogels were directly lysed on cell lysis buffer (RLT buffer, QIAGEN) and stored at -80°C until further processing.

Immunostaining and flow cytometry

For immunostaining, Fc blocking was performed using human IgG (Sigma-Aldrich) at a concentration of 4 µg/10^6 cells for 15 minutes at room temperature. Cells were stained with Human CD11b/Integrin alpha M Alexa Fluor® 405-conjugated Antibody (R&D Systems) at a concentration of 1 µg/10^6 cells according to manufacturer's protocols, using normal mouse IgG2b Alexa Fluor 405 (Santa Cruz Biotechnology) as isotype control. Flow cytometry was performed using a CellStream benchtop flow cytometer (Millipore Sigma). Single color controls were used to create a compensation matrix for signal bleed between fluorophores. Single cells were acquired using a 0.6-1 Aspect Ratio as the criterion. Dead

View Article Online
DOI: 10.1039/D5LC00052A

cells were excluded with Propidium Iodide (PI) staining (1.5 μM for 5 minutes). Mean Fluorescence Intensity per cell and cell counts were obtained directly from CellStream™ Software (Millipore Sigma).

Mammalian cell viability evaluation

Single cell suspensions were stained with 1.5 μM PI and incubated for 15 minutes in the dark at room temperature. Viability was evaluated using a Leica TCS SP5 confocal microscope. At least 100 cells were counted per sample, and 4 hydrogels were processed per treatment.

SCFA analysis

SCFA quantification was carried out by the Integrated Metabolomics Analysis Core at Texas A&M University. Metabolites were extracted from samples using ethyl acetate and the levels of 6 SCFAs (acetic, butyric, isobutyric, isovaleric, propionic, and valeric acid) were quantified using GC-MS. Isotopically labelled n-butyrate was used as the internal control and was spiked into all samples prior to extraction. Samples were diluted 10-fold in PBS before extraction. SCFAs were detected and quantified on a gas chromatography triple quadrupole mass spectrometer (TSQ EVO 8000, Thermo Scientific, Waltham, MA). Chromatographic separation was achieved on a ZB WAX Plus, 30 m x 0.25mm x 0.25 μm column (Phenomenex). The MS data and retention times were acquired in full scan mode from m/z 40-500 for the individual target compounds. The injector, MS transfer line and ion source were maintained at 230 °C, 240 °C and 240 °C respectively. The flow rate of helium carrier gas was kept at 1 mL/min. Samples were maintained at room temperature on an autosampler before injection. 1 μl of the extracted sample was injected with a split ratio of 20:1. The ionization was carried out in the electron impact (EI) mode at 70 eV. Sample acquisition and analysis was performed with TraceFinder 3.3 (Thermo Scientific).

Microbiota composition analysis

View Article Online
DOI: 10.1039/D5LC00052A

DNA from bacterial communities was extracted by using the DNeasy PowerSoil Kit (QIAGEN) according to manufacturer's instructions, and the v4 region of the 16S rRNA gene was sequenced using the MiSeq Illumina Platform (FERA Diagnostics and Biologicals). Bioinformatic analysis was performed using Microbiome Analyst (www.microbiomeanalyst.ca) at the genus level. Features with singlets were removed prior to analysis. Features with single readings were removed before analysis. For comparative analysis, only features with a read count higher than 4 in 50% of samples were included, and 10% of features with the lowest coefficient of variation were removed to ameliorate data sparsity and improve statistical power(92). Data was scaled using Cumulative Sum Scaling. The Bradis-Curtis Index distance metric was used with PERMANOVA as the statistical method. LEfSe analysis was performed using LDA > 2.0 as the significance filter and $p < 0.05$ was used for statistical significance.

Gene expression analysis

RNA was extracted from mammalian cells using the RNeasy Mini Kit (QIAGEN) following the manufacturer's instructions. Genomic DNA in the extracted RNA was eliminated by digesting with DNAse (QIAGEN). cDNA synthesis was performed using qScript™ cDNA SuperMix (QuantaBio) using 100 ng of RNA sample in a 10 µL reaction. Quantitative PCR was carried out in a Lightcycler® 96 (Roche) using FastStart Universal SYBR Green Master (Roche). Primers were designed using Primer Blast (NCBI), and amplicon size and specificity were confirmed by melting peak analysis and agarose gel electrophoresis of the reaction products. Each reaction mix contained $1/40^{th}$ of the cDNA pool obtained per sample and a total primer concentration of 400 nM. The PCR regime consisted of preincubation for 10 minutes at 95 °C and 45 amplification cycles (95 °C x 15 s, 65 °C x 30 s, 72 °C x 45 s). Data were processed using the $2^{-\Delta\Delta Ct}$ method. Multiple genes were evaluated as endogenous qPCR controls, including *18s*, *YWHAZ*, *PMM1*, *UBC*, *IPO8*, and *VPS29*; from these genes, *PMM1* showed the most stable

View Article Online
DOI: 10.1039/D5LC00052A

expression level and was employed as endogenous control. Sequences for all used primers are provided in **Table 1**.

Table 1 Primer sequences for gene expression analysis.

Gene	Forward Primer	Reverse Primer
PMM1	GTGTTCCCCATGCTCCACCT	ATAGGCACCTTCCCCACCGT
TNF-α	CTCTTCTGCCTGCTGCQCTTTG	ATGGGCTACAGGCTTGTCACTC
CD80	CTCTTGGTGCTGGCTGGTCTTT	GCCAGTAGATGCGAGTTTGTGC
CD44	CCAGAAGGAACAGTGGTTTGGC	ACTGTCCTCTGGGCTTGGTGTT
CD40	CCTGTTTGCCATCCTCTTGGTG	AGCAGTGTTGGAGCCAGGAAGA
CD11b	GGAACGCCATTGTCTGCTTTCG	ATGCTGAGGTCATCCTGGCAGA
CD86	CTGCTCATCTATACACGGTTACC	GGAACGTCGTACAGTTCTGTG
CD68	CTTCTCTCATTCCCCTATGGACA	GAAGGACACATTGTACTCCACC
CD206	GGGTTGCTATCACTCTCTATGC	TTTCTTGTCTGTTGCCGTAGTT
CD163	TTTGTCAACTTGAGTCCCTTCAC	TCCCGCTACACTTGTTTTCAC

Statistical analysis

For testing statistical significance, unpaired Student's t-tests were performed on sets of data with two experimental conditions. One-way ANOVAs were used for comparisons among multiple experimental conditions and during RTqPCR data analysis. For RTqPCR data analysis, significance in gene expression changes was determined by comparing ΔCt values across treatments, as gene expression data is log normally distributed(93). The assumption of equality of variances among data sets was confirmed by using the Levene's test, and normality was validated using the Shapiro-Wilk test. All experiments were performed at least in duplicate, and coculture experiments were performed in triplicate.

Effect of SCFA on cytokine production during transwell co-cultures

View Article Online
DOI: 10.1039/D5LC00052A

To study the effect of SCFA on the THP-1 and HCT116 co-culture, 50 uL of Matrigel containing ~2.5x10^6 cell/mL of HCT 116 and ~2.5x10^6 cell/mL of THP-1 were seeded in a 24 well transwell plate in the well and the insert, respectively. RPMI media containing 50 ng/mL PMA was added to the well (600 μL) and insert (300 μL) and kept in co-culture. After 72 hours, the plate was transferred in an anaerobic chamber and the media replaced with fresh RPMI media with PMA. The THP-1 containing transwells were either shifted to a different well, to study the individual culture or kept in the co-culture for 24 hours. Cells were then treated for 12 hours with RPMI medium containing sodium acetate, sodium butyrate, and sodium propionate at concentrations previously measured in device co-cultures (μM): 234.6, 12.1, 50.5 ("Inulin-negative SCFA"); 12.55, 6.7, 63.3 ("Inulin-derived SCFA"), respectively. Cell supernatants were collected and stored at -80°C for cytokine analysis.

Multiplex Cytokine analysis

Stored cell supernatants were centrifuged at 300 x *g* for 4 min to remove cell debris and the supernatant was then analyzed for a panel of 13 inflammatory cytokines using the LegendPlex Human Inflammation Panel (13-Plex), according to manufacturer's instructions. Samples were analyzed via flow cytometry using a Cytek Aurora Spectral Flow Cytometer (Cytek Biosciences).

Author contributions

D. P., M. M., and A. J. designed the research. D. P. and M. M. performed the experiments. D. P., M. M., S. C., A. H. and A. J. analyzed the data. D. P., M. M., and A. J. wrote the article with input from A. H and S. C. All authors reviewed, discussed, and edited the manuscript.

View Article Online
DOI: 10.1039/D5LC00052A

Conflicts of interest

The authors declare that they do not have any competing interests.

Acknowledgements

This work was partially supported by funds from the Ray B. Nesbitt Chair endowment to A. J. The authors acknowledge use of facilities at the Integrated Metabolomics Analysis Core (IMACT) at Texas A&M University.

References

1. Veettil SK, Wong TY, Loo YS, Playdon MC, Lai NM, Giovannucci EL, et al. Role of Diet in Colorectal Cancer Incidence: Umbrella Review of Meta-analyses of Prospective Observational Studies. JAMA Netw Open [Internet]. 2021 Feb 16 [cited 2022 Aug 4]; 4(2):e2037341. Available from: https://doi.org/10.1001/jamanetworkopen.2020.37341

2. Pool-Zobel BL. Inulin-type fructans and reduction in colon cancer risk: review of experimental and human data. Br J Nutr. 2005 Apr [cited 2022 Aug 4]; 93 Suppl 1:S73-90. Available from: https://doi.org/10.1079/bjn20041349

3. So D, Whelan K, Rossi M, Morrison M, Holtmann G, Kelly JT, et al. Dietary fiber intervention on gut microbiota composition in healthy adults: a systematic review and meta-analysis. Am J Clin Nutr. 2018 Jun 1 [cited 2022 Aug 4]; 107(6):965–83. Available from: https://doi.org/10.1093/ajcn/nqy041

4. Bishehsari F, Engen PA, Preite NZ, Tuncil YE, Naqib A, Shaikh M, et al. Dietary Fiber Treatment Corrects the Composition of Gut Microbiota, Promotes SCFA Production, and Suppresses Colon Carcinogenesis. Genes. 2018 Feb 16 [cited 2022 Aug 4]; 9(2). Available from: https://doi.org/10.3390/genes9020102

5. Makki K, Deehan EC, Walter J, Bäckhed F. The Impact of Dietary Fiber on Gut Microbiota in Host Health and Disease. Cell Host Microbe [Internet]. 2018 Jun 13 [cited 2022 Aug 18]; 23(6):705–15. Available from: https://doi.org/10.1016/j.chom.2018.05.012

6. Wu X, Wu Y, He L, Wu L, Wang X, Liu Z. Effects of the intestinal microbial metabolite butyrate on the development of colorectal cancer. J Cancer [Internet]. 2018 Jun 15 [cited 2020 Apr 9]; 9(14):2510–7. Available from: https://doi.org/10.7150/jca.25324

View Article Online
DOI: 10.1039/D5LC00052A

7. Waldecker M, Kautenburger T, Daumann H, Busch C, Schrenk D. Inhibition of histone-deacetylase activity by short-chain fatty acids and some polyphenol metabolites formed in the colon. J Nutr Biochem. 2008 Sep [cited 2020 Apr 9]; 19(9):587–93. Available from: https://doi.org/10.1016/j.jnutbio.2007.08.002

8. Sahuri-Arisoylu M, Mould RR, Shinjyo N, Bligh SWA, Nunn AVW, Guy GW, et al. Acetate Induces Growth Arrest in Colon Cancer Cells Through Modulation of Mitochondrial Function. Front Nutr [Internet]. 2021 Apr 15 [cited 2022 Aug 18]; 8:588466. Available from: https://doi.org/10.3389/fnut.2021.588466

9. Oliveira CSF, Pereira H, Alves S, Castro L, Baltazar F, Chaves SR, et al. Cathepsin D protects colorectal cancer cells from acetate-induced apoptosis through autophagy-independent degradation of damaged mitochondria. Cell Death Dis [Internet]. 2015 Jun [cited 2022 Aug 18]; 6(6):e1788–e1788. Available from: https://doi.org/10.1038/cddis.2015.157

10. Marques C, Oliveira CSF, Alves S, Chaves SR, Coutinho OP, Côrte-Real M, et al. Acetate-induced apoptosis in colorectal carcinoma cells involves lysosomal membrane permeabilization and cathepsin D release. Cell Death Dis [Internet]. 2013 Feb [cited 2022 Aug 18]; 4(2):e507–e507. Available from: https://doi.org/10.1038/cddis.2013.29

11. Ryu TY, Kim K, Son M-Y, Min J-K, Kim J, Han T-S, et al. Downregulation of PRMT1, a histone arginine methyltransferase, by sodium propionate induces cell apoptosis in colon cancer. Oncol Rep [Internet]. 2019 Mar 1 [cited 2022 Aug 18]; 41(3):1691–9. Available from: https://doi.org/10.3892/or.2018.6938

12. Liong M-T. Roles of Probiotics and Prebiotics in Colon Cancer Prevention: Postulated Mechanisms and In-vivo Evidence. Int J Mol Sci [Internet]. 2008 May 20 [cited 2022 Aug 22]; 9(5):854–63. Available from: https://doi.org/10.3390/ijms9050854 PMID: 19325789

13. Li J, Chen D, Shen M. Tumor Microenvironment Shapes Colorectal Cancer Progression, Metastasis, and Treatment Responses. Front Med [Internet]. 2022 Mar [cited 2022 Jun 22];9.

14. van Ravenswaay Claasen HH, Kluin PM, Fleuren GJ. Tumor infiltrating cells in human cancer. On the possible role of CD16+ macrophages in antitumor cytotoxicity. Lab Investig J Tech Methods Pathol. 1992 Aug [cited 2022 Jun 22]; 67(2):166–74.

15. McBride WH. Phenotype and functions of intratumoral macrophages. Biochim Biophys Acta BBA - Rev Cancer [Internet]. 1986 Aug 5 [cited 2022 Jul 30]; 865(1):27–41. Available from: https://doi.org/10.1016/0304-419X(86)90011-9

16. Luput L, Licarete E, Sesarman A, Patras L, Alupei MC, Banciu M. Tumor-associated macrophages favor C26 murine colon carcinoma cell proliferation in an oxidative stress-dependent manner. Oncol Rep. 2017 Apr [cited 2022 Jul 30]; 37(4):2472–80. Available from: https://doi.org/10.3892/or.2017.5466

View Article Online
DOI: 10.1039/D5LC00052A

17. Miao H, Ou J, Peng Y, Zhang X, Chen Y, Hao L, et al. Macrophage ABHD5 promotes colorectal cancer growth by suppressing spermidine production by SRM. Nat Commun [Internet]. 2016 May 18 [cited 2022 Jul 31]; 7:11716. Available from: https://doi.org/10.1038/ncomms11716

18. Lan J, Sun L, Xu F, Liu L, Hu F, Song D, et al. M2 Macrophage-Derived Exosomes Promote Cell Migration and Invasion in Colon Cancer. Cancer Res. 2019 Jan 1 [cited 2022 Aug 22]; 79(1):146–58. Available from: https://doi.org/10.1158/0008-5472.CAN-18-0014

19. Jedinak A, Dudhgaonkar S, Sliva D. Activated macrophages induce metastatic behavior of colon cancer cells. Immunobiology. 2010 Mar [cited 2022 Aug 22]; 215(3):242–9. Available from: https://doi.org/10.1016/j.imbio.2009.03.004

20. Vinnakota K, Zhang Y, Selvanesan BC, Topi G, Salim T, Sand-Dejmek J, et al. M2-like macrophages induce colon cancer cell invasion via matrix metalloproteinases. J Cell Physiol. 2017 Dec [cited 2022 Aug 22]; 232(12):3468–80. Available from: https://doi.org/10.1002/jcp.25808

21. Wang X, Lin Y. Tumor necrosis factor and cancer, buddies or foes? Acta Pharmacol Sin [Internet]. 2008 Nov [cited 2022 Aug 22]; 29(11):1275–88. Available from: https://doi.org/10.1111/j.1745-7254.2008.00889.x

22. de Looff M, de Jong S, Kruyt FAE. Multiple Interactions Between Cancer Cells and the Tumor Microenvironment Modulate TRAIL Signaling: Implications for TRAIL Receptor Targeted Therapy. Front Immunol [Internet]. 2019 Jul 3 [cited 2022 Jun 22]; 10:1530. Available from: https://doi.org/10.3389/fimmu.2019.01530

23. Baay M, Brouwer A, Pauwels P, Peeters M, Lardon F. Tumor Cells and Tumor-Associated Macrophages: Secreted Proteins as Potential Targets for Therapy. Clin Dev Immunol [Internet]. 2011 [cited 2022 Aug 1]; 2011:565187. Available from: https://doi.org/10.1155/2011/565187

24. Han C, Zhang C, Wang H, Zhao L. Exosome-mediated communication between tumor cells and tumor-associated macrophages: implications for tumor microenvironment. Oncoimmunology. 2021 Feb 22 [cited 2022 Aug 22]; 10(1):1887552. Available from: https://doi.org/10.1080/2162402X.2021.1887552

25. Chen Q, Nair S, Ruedl C. Microbiota regulates the turnover kinetics of gut macrophages in health and inflammation. Life Sci Alliance [Internet]. 2022 Jan 1 [cited 2022 Aug 18]; 5(1). Available from: https://doi.org/10.26508/lsa.202101178

26. Mola S, Pandolfo C, Sica A, Porta C. The Macrophages-Microbiota Interplay in Colorectal Cancer (CRC)-Related Inflammation: Prognostic and Therapeutic Significance. Int J Mol Sci [Internet]. 2020 Sep 18 [cited 2022 Aug 18];21(18):6866. Available from: https://doi.org/10.3390/ijms21186866

27. Fang H, Pengal RA, Cao X, Ganesan LP, Wewers MD, Marsh CB, et al. Lipopolysaccharide-induced macrophage inflammatory response is regulated by SHIP. J Immunol Baltim Md 1950.

View Article Online
DOI: 10.1039/D5LC00052A

2004 Jul 1 [cited 2020 Apr 19]; 173(1):360–6. Available from: https://doi.org/10.4049/jimmunol.173.1.360

28. Ji J, Shu D, Zheng M, Wang J, Luo C, Wang Y, et al. Microbial metabolite butyrate facilitates M2 macrophage polarization and function. Sci Rep [Internet]. 2016 Apr 20 [cited 2020 Apr 19]; 6(1):1–10. Available from: https://doi.org/10.1038/srep24838

29. Schulthess J, Pandey S, Capitani M, Rue-Albrecht KC, Arnold I, Franchini F, et al. The Short Chain Fatty Acid Butyrate Imprints an Antimicrobial Program in Macrophages. Immunity. 2019 Feb 19 [cited 2020 Apr 19]; 50(2):432-445.e7. Available from: https://doi.org/10.1016/j.immuni.2018.12.018

30. Pleguezuelos-Manzano C, Puschhof J, Rosendahl Huber A, van Hoeck A, Wood HM, Nomburg J, et al. Mutational signature in colorectal cancer caused by genotoxic pks+ E. coli. Nature. 2020 Apr [cited 2020 Apr 19]; 580(7802):269–73. Available from: https://doi.org/10.1038/s41586-020-2080-8

31. Kim HJ, Li H, Collins JJ, Ingber DE. Contributions of microbiome and mechanical deformation to intestinal bacterial overgrowth and inflammation in a human gut-on-a-chip. Proc Natl Acad Sci U S A. 2016 Jan 5 [cited 2020 Apr 19]; 113(1):E7-15. Available from: https://doi.org/10.1073/pnas.1522193112

32. Greenhalgh K, Ramiro-Garcia J, Heinken A, Ullmann P, Bintener T, Pacheco MP, et al. Integrated In Vitro and In Silico Modeling Delineates the Molecular Effects of a Synbiotic Regimen on Colorectal-Cancer-Derived Cells. Cell Rep. 2019 Apr 30 [cited 2020 Apr 19]; 27(5):1621-1632.e9. Available from: https://doi.org/10.1016/j.celrep.2019.04.001

33. Penarete-Acosta D, Stading R, Emerson L, Horn M, Chakraborty S, Han A, et al. A microfluidic co-culture model for investigating colonocytes–microbiota interactions in colorectal cancer. Lab Chip [Internet]. 2024 Jul 23 [cited 2024 Sep 28]; 24(15):3690–703. Available from: https://doi.org/10.1039/D4LC00013G

34. Park EK, Jung HS, Yang HI, Yoo MC, Kim C, Kim KS. Optimized THP-1 differentiation is required for the detection of responses to weak stimuli. Inflamm Res Off J Eur Histamine Res Soc Al. 2007 Jan [cited 2022 Aug 15]; 56(1):45–50. Available from: https://doi.org/10.1007/s00011-007-6115-5

35. Starr T, Bauler TJ, Malik-Kale P, Steele-Mortimer O. The phorbol 12-myristate-13-acetate differentiation protocol is critical to the interaction of THP-1 macrophages with Salmonella Typhimurium. PLOS ONE [Internet]. 2018 Mar 14 [cited 2022 Aug 15];13(3):e0193601. Available from: https://doi.org/10.1371/journal.pone.0193601

36. Lund ME, To J, O'Brien BA, Donnelly S. The choice of phorbol 12-myristate 13-acetate differentiation protocol influences the response of THP-1 macrophages to a pro-inflammatory stimulus. J Immunol Methods. 2016 Mar [cited 2022 Aug 16]; 430:64–70. Available from: https://doi.org/10.1016/j.jim.2016.01.012

View Article Online
DOI: 10.1039/D5LC00052A

37. Ma Y, Hu M, Zhou L, Ling S, Li Y, Kong B, et al. Dietary fiber intake and risks of proximal and distal colon cancers: A meta-analysis. Medicine (Baltimore). 2018 Sep [cited 2022 Aug 16]; 97(36):e11678. Available from: https://doi.org/10.1097/MD.0000000000011678

38. Pool-Zobel BL, Sauer J. Overview of Experimental Data on Reduction of Colorectal Cancer Risk by Inulin-Type Fructans. J Nutr [Internet]. 2007 Nov 1 [cited 2022 Aug 16]; 137(11):2580S-2584S. Available from: https://doi.org/10.1093/jn/137.11.2580S

39. Cummings JH, Macfarlane GT, Englyst HN. Prebiotic digestion and fermentation. Am J Clin Nutr [Internet]. 2001 Feb 1 [cited 2022 Aug 16]; 73(2):415s–20s. Available from: https://doi.org/10.1093/ajcn/73.2.415s

40. Xiao J, Metzler-Zebeli BU, Zebeli Q. Gut Function-Enhancing Properties and Metabolic Effects of Dietary Indigestible Sugars in Rodents and Rabbits. Nutrients [Internet]. 2015 Sep 28 [cited 2022 Aug 16]; 7(10):8348–65. Available from: https://doi.org/10.3390/nu7105397

41. Falony G, Calmeyn T, Leroy F, De Vuyst L. Coculture Fermentations of Bifidobacterium Species and Bacteroides thetaiotaomicron Reveal a Mechanistic Insight into the Prebiotic Effect of Inulin-Type Fructans. Appl Environ Microbiol [Internet]. 2009 Apr 15 [cited 2022 Sep 7]; 75(8):2312–9. Available from: https://doi.org/10.1128/AEM.02649-08

42. Hiel S, Gianfrancesco MA, Rodriguez J, Portheault D, Leyrolle Q, Bindels LB, et al. Link between gut microbiota and health outcomes in inulin -treated obese patients: Lessons from the Food4Gut multicenter randomized placebo-controlled trial. Clin Nutr [Internet]. 2020 Dec 1 [cited 2022 Sep 7]; 39(12):3618–28. Available from: https://doi.org/10.1016/j.clnu.2020.04.005

43. Vandeputte D, Falony G, Vieira-Silva S, Wang J, Sailer M, Theis S, et al. Prebiotic inulin-type fructans induce specific changes in the human gut microbiota. Gut [Internet]. 2017 Nov 1 [cited 2022 Aug 25]; 66(11):1968–74. Available from: https://doi.org/10.1136/gutjnl-2016-313271

44. Le Bastard Q, Chapelet G, Javaudin F, Lepelletier D, Batard E, Montassier E. The effects of inulin on gut microbial composition: a systematic review of evidence from human studies. Eur J Clin Microbiol Infect Dis [Internet]. 2020 Mar 1 [cited 2022 Aug 25]; 39(3):403–13. Available from: https://doi.org/10.1007/s10096-019-03721-w

45. Wang X, Wang T, Zhang Q, Xu L, Xiao X. Dietary Supplementation with Inulin Modulates the Gut Microbiota and Improves Insulin Sensitivity in Prediabetes. Int J Endocrinol. 2021 [cited 2022 Aug 25]; 2021:5579369. Available from: https://doi.org/10.1155/2021/5579369

46. Fernández J, Ledesma E, Monte J, Millán E, Costa P, de la Fuente VG, et al. Traditional Processed Meat Products Re-designed Towards Inulin-rich Functional Foods Reduce Polyps in Two Colorectal Cancer Animal Models. Sci Rep. 2019 Oct 15 [cited 2022 Aug 25]; 9(1):14783. Available from: https://doi.org/10.1038/s41598-019-51437-w

47. Rao CV, Chou D, Simi B, Ku H, Reddy BS. Prevention of colonic aberrant crypt foci and modulation of large bowel microbial activity by dietary coffee fiber, inulin and pectin.

View Article Online
DOI: 10.1039/D5LC00052A

Carcinogenesis. 1998 Oct [cited 2022 Aug 25]; 19(10):1815–9. Available from: https://doi.org/10.1093/carcin/19.10.1815

48. Poulsen M, Mølck A-M, Jacobsen BL. Different effects of short- and long-chained fructans on large intestinal physiology and carcinogen-induced aberrant crypt foci in rats. Nutr Cancer. 2002 [cited 2022 Aug 25]; 42(2):194–205. Available from: https://doi.org/10.1207/S15327914NC422_8

49. Femia AP, Luceri C, Dolara P, Giannini A, Biggeri A, Salvadori M, et al. Antitumorigenic activity of the prebiotic inulin enriched with oligofructose in combination with the probiotics Lactobacillus rhamnosus and Bifidobacterium lactis on azoxymethane-induced colon carcinogenesis in rats. Carcinogenesis. 2002 Nov [cited 2022 Aug 25]; 23(11):1953–60. Available from: https://doi.org/10.1093/carcin/23.11.1953

50. Wang Z, Zhang X, Zhu L, Yang X, He F, Wang T, et al. Inulin alleviates inflammation of alcoholic liver disease via SCFAs-inducing suppression of M1 and facilitation of M2 macrophages in mice. Int Immunopharmacol. 2019 Dec 9 [cited 2022 Aug 25]; 78:106062. Available from: https://doi.org/10.1016/j.intimp.2019.106062

51. Nakajima H, Nakanishi N, Miyoshi T, Okamura T, Hashimoto Y, Senmaru T, et al. Inulin reduces visceral adipose tissue mass and improves glucose tolerance through altering gut metabolites. Nutr Metab [Internet]. 2022 Jul 28 [cited 2022 Aug 18];19(1):50. Available from: https://doi.org/10.1186/s12986-022-00685-1

52. Rios-Covian D, Salazar N, Gueimonde M, de los Reyes-Gavilan CG. Shaping the Metabolism of Intestinal Bacteroides Population through Diet to Improve Human Health. Front Microbiol [Internet]. 2017 [cited 2022 Sep 7]; 7(8):376.

53. Louis P, Flint HJ. Formation of propionate and butyrate by the human colonic microbiota. Environ Microbiol [Internet]. 2017 [cited 2022 Sep 7]; 19(1):29–41. Available from: https://doi.org/10.1111/1462-2920.13589

54. De Mets F, Van Melderen L, Gottesman S. Regulation of acetate metabolism and coordination with the TCA cycle via a processed small RNA. Proc Natl Acad Sci [Internet]. 2019 Jan 15 [cited 2022 Aug 27]; 116(3):1043–52. Available from: https://doi.org/10.1073/pnas.1815288116

55. Lee HL, Shen H, Hwang IY, Ling H, Yew WS, Lee YS, et al. Targeted Approaches for In Situ Gut Microbiome Manipulation. Genes [Internet]. 2018 Jul 12 [cited 2022 Aug 19]; 9(7):351. Available from: https://doi.org/10.3390/genes9070351

56. Birkeland E, Gharagozlian S, Birkeland KI, Valeur J, Måge I, Rud I, et al. Prebiotic effect of inulin-type fructans on faecal microbiota and short-chain fatty acids in type 2 diabetes: a randomised controlled trial. Eur J Nutr [Internet]. 2020 Oct 1 [cited 2022 Aug 18]; 59(7):3325–38. Available from: https://doi.org/10.1007/s00394-020-02282-5

57. Poeker SA, Lacroix C, de Wouters T, Spalinger MR, Scharl M, Geirnaert A. Stepwise Development of an in vitro Continuous Fermentation Model for the Murine Caecal Microbiota.

View Article Online
DOI: 10.1039/D5LC00052A

Front Microbiol [Internet]. 2019 [cited 2020 Apr 10]; 29(10):1166. Available from: https://doi.org/10.3389/fmicb.2019.01166

58. Holmes ZC, Villa MM, Durand HK, Jiang S, Dallow EP, Petrone BL, et al. Microbiota responses to different prebiotics are conserved within individuals and associated with habitual fiber intake. Microbiome [Internet]. 2022 Jul 29 [cited 2022 Aug 19]; 10(1):114. Available from: https://doi.org/10.1186/s40168-022-01307-x

59. Donohoe DR, Holley D, Collins LB, Montgomery SA, Whitmore AC, Hillhouse A, et al. A Gnotobiotic Mouse Model Demonstrates that Dietary Fiber Protects Against Colorectal Tumorigenesis in a Microbiota- and Butyrate–Dependent Manner. Cancer Discov [Internet]. 2014 Dec [cited 2022 Jul 16]; 4(12):1387–97. Available from: https://doi.org/10.1158/2159-8290.CD-14-0501

60. Fan R, Naqvi K, Patel K, Sun J, Wan J. Evaporation-based microfluidic production of oil-free cell-containing hydrogel particles. Biomicrofluidics [Internet]. 2015 Mar 27 [cited 2022 Aug 27]; 9(5):052602. Available from: https://doi.org/10.1063/1.4916508

61. Wilson CA, Browning JL. Death of HT29 adenocarcinoma cells induced by TNF family receptor activation is caspase-independent and displays features of both apoptosis and necrosis. Cell Death Differ. 2002 Dec [cited 2022 Aug 25]; 9(12):1321–33. Available from: https://doi.org/10.1038/sj.cdd.4401107

62. Eslick S, Williams EJ, Berthon BS, Wright T, Karihaloo C, Gately M, et al. Weight Loss and Short-Chain Fatty Acids Reduce Systemic Inflammation in Monocytes and Adipose Tissue Macrophages from Obese Subjects. Nutrients. 2022 Feb 11 [cited 2022 Aug 25]; 14(4):765. Available from: https://doi.org/10.3390/nu14040765

63. Gazzaniga S, Bravo AI, Guglielmotti A, van Rooijen N, Maschi F, Vecchi A, et al. Targeting Tumor-Associated Macrophages and Inhibition of MCP-1 Reduce Angiogenesis and Tumor Growth in a Human Melanoma Xenograft. J Invest Dermatol [Internet]. 2007 Aug 1 [cited 2025 Jan 5]; 127(8):2031–41. Available from: https://doi.org/10.1038/sj.jid.5700827

64. Fousek K, Horn LA, Palena C. Interleukin-8: A chemokine at the intersection of cancer plasticity, angiogenesis, and immune suppression. Pharmacol Ther [Internet]. 2021 Mar 1 [cited 2025 Jan 5]; 219:107692. Available from: https://doi.org/10.1016/j.pharmthera.2020.107692

65. Sun R, Abraham C. IL23 Promotes Antimicrobial Pathways in Human Macrophages, Which Are Reduced With the IBD-Protective IL23R R381Q Variant. Cell Mol Gastroenterol Hepatol. 2020 [cited 2022 Aug 25]; 10(4):673–97. Available from: https://doi.org/10.1016/j.jcmgh.2020.05.007

66. Sun R, Hedl M, Abraham C. IL23 induces IL23R recycling and amplifies innate receptor-induced signalling and cytokines in human macrophages, and the IBD-protective IL23R R381Q variant modulates these outcomes. Gut [Internet]. 2020 Feb [cited 2025 Jan 5]; 69(2):264–73. Available from: https://doi.org/10.1136/gutjnl-2018-316830

View Article Online
DOI: 10.1039/D5LC00052A

67. Jorgovanovic D, Song M, Wang L, Zhang Y. Roles of IFN-γ in tumor progression and regression: a review. Biomark Res [Internet]. 2020 Sep 29 [cited 2025 Jan 5]; 29(8):49. Available from: https://doi.org/10.1186/s40364-020-00228-x

68. Bastos KRB, Marinho CRF, Barboza R, Russo M, Álvarez JM, D'Império Lima MR. What kind of message does IL-12/IL-23 bring to macrophages and dendritic cells? Microbes Infect [Internet]. 2004 May 1 [cited 2025 Jan 5]; 6(6):630–6. Available from: https://doi.org/10.1016/j.micinf.2004.02.012

69. Masztalerz A, Van Rooijen N, Den Otter W, Everse LA. Mechanisms of macrophage cytotoxicity in IL-2 and IL-12 mediated tumour regression. Cancer Immunol Immunother CII [Internet]. 2003 Apr [cited 2025 Jan 5]; 52(4):235–42. Available from: https://doi.org/10.1007/s00262-003-0381-z

70. Yan J, Smyth MJ, Teng MWL. Interleukin (IL)-12 and IL-23 and Their Conflicting Roles in Cancer. Cold Spring Harb Perspect Biol [Internet]. 2018 Jul [cited 2025 Jan 5]; 10(7):a028530. Available from: https://doi.org/10.1101/cshperspect.a028530

71. Inhibition of IL-8 Receptor Reduces Colorectal Cancer Proliferation - The ASCO Post [Internet]. [cited 2021 Jul 13]. Available from: https://ascopost.com/issues/may-15-2012/inhibition-of-il-8-receptor-reduces-colorectal-cancer-proliferation/

72. Krishnan S, Ding Y, Saedi N, Choi M, Sridharan GV, Sherr DH, et al. Gut Microbiota-Derived Tryptophan Metabolites Modulate Inflammatory Response in Hepatocytes and Macrophages. Cell Rep [Internet]. 2018 Apr 24 [cited 2022 Oct 7]; 23(4):1099–111. Available from: https://doi.org/10.1016/j.celrep.2018.03.109

73. O'Keefe SJD. Diet, microorganisms and their metabolites, and colon cancer. Nat Rev Gastroenterol Hepatol. 2016 Dec [cited 2022 Aug 25]; 13(12):691–706. Available from: https://doi.org/10.1038/nrgastro.2016.165

74. Fung KYC, Brierley GV, Henderson S, Hoffmann P, McColl SR, Lockett T, et al. Butyrate-induced apoptosis in HCT116 colorectal cancer cells includes induction of a cell stress response. J Proteome Res. 2011 Apr 1 [cited 2022 Aug 25]; 10(4):1860–9. Available from: https://doi.org/10.1021/pr1011125

75. Ramirez-Farias C, Slezak K, Fuller Z, Duncan A, Holtrop G, Louis P. Effect of inulin on the human gut microbiota: stimulation of Bifidobacterium adolescentis and Faecalibacterium prausnitzii. Br J Nutr [Internet]. 2008 Jul [cited 2022 Aug 25]; 101(4):541–50. Available from: https://doi.org/10.1017/S0007114508019880

76. Baxter NT, Schmidt AW, Venkataraman A, Kim KS, Waldron C, Schmidt TM. Dynamics of Human Gut Microbiota and Short-Chain Fatty Acids in Response to Dietary Interventions with Three Fermentable Fibers. mBio. 2019 Jan 29 [cited 2022 Aug 25]; 10(1):e02566-18. Available from: https://doi.org/10.1128/mBio.02566-18

View Article Online
DOI: 10.1039/D5LC00052A

77. Salazar N, Dewulf EM, Neyrinck AM, Bindels LB, Cani PD, Mahillon J, et al. Inulin-type fructans modulate intestinal Bifidobacterium species populations and decrease fecal short-chain fatty acids in obese women. Clin Nutr [Internet]. 2015 Jun 1 [cited 2022 Aug 25]; 34(3):501–7. Available from: https://doi.org/10.1016/j.clnu.2014.06.001

78. Healey G, Murphy R, Butts C, Brough L, Whelan K, Coad J. Habitual dietary fibre intake influences gut microbiota response to an inulin-type fructan prebiotic: a randomised, double-blind, placebo-controlled, cross-over, human intervention study. Br J Nutr [Internet]. 2018 Jan [cited 2022 Aug 25]; 119(2):176–89. Available from: https://doi.org/10.1017/S0007114517003440

79. Liu F, Li P, Chen M, Luo Y, Prabhakar M, Zheng H, et al. Fructooligosaccharide (FOS) and Galactooligosaccharide (GOS) Increase Bifidobacterium but Reduce Butyrate Producing Bacteria with Adverse Glycemic Metabolism in healthy young population. Sci Rep [Internet]. 2017 Sep 18 [cited 2022 Aug 25]; 7(1):11789. Available from: https://doi.org/10.1038/s41598-017-10722-2

80. Holscher HD, Bauer LL, Gourineni V, Pelkman CL, Fahey GC Jr, Swanson KS. Agave Inulin Supplementation Affects the Fecal Microbiota of Healthy Adults Participating in a Randomized, Double-Blind, Placebo-Controlled, Crossover Trial. J Nutr [Internet]. 2015 Sep 1 [cited 2022 Aug 25]; 145(9):2025–32. Available from: https://doi.org/10.3945/jn.115.217331

81. Roller M, Pietro Femia A, Caderni G, Rechkemmer G, Watzl B. Intestinal immunity of rats with colon cancer is modulated by oligofructose-enriched inulin combined with Lactobacillus rhamnosus and Bifidobacterium lactis. Br J Nutr. 2004 Dec [cited 2022 Aug 25]; 92(6):931–8. Available from: https://doi.org/10.1079/bjn20041289

82. Li Y, Elmén L, Segota I, Xian Y, Tinoco R, Feng Y, et al. Prebiotic-Induced Anti-tumor Immunity Attenuates Tumor Growth. Cell Rep. 2020 Feb 11 [cited 2022 Aug 25]; 30(6):1753-1766.e6. Available from: https://doi.org/10.1016/j.celrep.2020.01.035

83. Braster R, Bögels M, Beelen RHJ, van Egmond M. The delicate balance of macrophages in colorectal cancer; their role in tumour development and therapeutic potential. Immunobiology. 2017 [cited 2022 Aug 25]; 222(1):21–30. Available from: https://doi.org/10.1016/j.imbio.2015.08.011

84. Zhong X, Chen B, Yang Z. The Role of Tumor-Associated Macrophages in Colorectal Carcinoma Progression. Cell Physiol Biochem [Internet]. 2018 [cited 2022 Jul 31]; 45(1):356–65. Available from: https://doi.org/10.1159/000486816

85. Li J, Li L, Li Y, Long Y, Zhao Q, Ouyang Y, et al. Tumor-associated macrophage infiltration and prognosis in colorectal cancer: systematic review and meta-analysis. Int J Colorectal Dis [Internet]. 2020 Jul 1 [cited 2022 Jul 31]; 35(7):1203–10. Available from: https://doi.org/10.1007/s00384-020-03593-z

86. Bein A, Shin W, Jalili-Firoozinezhad S, Park MH, Sontheimer-Phelps A, Tovaglieri A, et al. Microfluidic Organ-on-a-Chip Models of Human Intestine. Cell Mol Gastroenterol Hepatol. 2018 [cited 2022 Aug 25]; 5(4):659–68. Available from: https://doi.org/10.1016/j.jcmgh.2017.12.010

View Article Online
DOI: 10.1039/D5LC00052A

87. Falony G, Lazidou K, Verschaeren A, Weckx S, Maes D, De Vuyst L. In Vitro Kinetic Analysis of Fermentation of Prebiotic Inulin-Type Fructans by Bifidobacterium Species Reveals Four Different Phenotypes. Appl Environ Microbiol [Internet]. 2009 Jan [cited 2025 May 25]; 75(2):454–61. Available from: https://doi.org/10.1128/AEM.01488-08

88. Logtenberg MJ, Akkerman R, An R, Hermes GDA, de Haan BJ, Faas MM, et al. Fermentation of Chicory Fructo-Oligosaccharides and Native Inulin by Infant Fecal Microbiota Attenuates Pro-Inflammatory Responses in Immature Dendritic Cells in an Infant-Age-Dependent and Fructan-Specific Way. Mol Nutr Food Res [Internet]. 2020 Jul [cited 2025 May 25]; 64(13):2000068. Available from: https://doi.org/10.1002/mnfr.202000068

89. Zhang N, Wang Z, Zhao Y. Selective inhibition of Tumor necrosis factor receptor-1 (TNFR1) for the treatment of autoimmune diseases. Cytokine Growth Factor Rev [Internet]. 2020 Oct 1 [cited 2022 Aug 27]; 55:80–5. Available from: https://doi.org/10.1016/j.cytogfr.2020.03.002

90. Covarrubias S, Vollmers AC, Capili A, Boettcher M, Shulkin A, Correa MR, et al. High-Throughput CRISPR Screening Identifies Genes Involved in Macrophage Viability and Inflammatory Pathways. Cell Rep [Internet]. 2020 Dec [cited 2022 Aug 27]; 33(13):108541. Available from: https://doi.org/10.1016/j.celrep.2020.108541

91. Tedesco S, De Majo F, Kim J, Trenti A, Trevisi L, Fadini GP, et al. Convenience versus Biological Significance: Are PMA-Differentiated THP-1 Cells a Reliable Substitute for Blood-Derived Macrophages When Studying in Vitro Polarization? Front Pharmacol. 2018 Dec [cited 2022 Aug 27]; 9:71. Available from: https://doi.org/10.3389/fphar.2018.00071

92. Dhariwal A, Chong J, Habib S, King IL, Agellon LB, Xia J. MicrobiomeAnalyst: a web-based tool for comprehensive statistical, visual and meta-analysis of microbiome data. Nucleic Acids Res [Internet]. 2017 Jul 3 [cited 2022 Sep 3]; 45(W1):W180–8. Available from: https://doi.org/10.1093/nar/gkx295

93. Derveaux S, Vandesompele J, Hellemans J. How to do successful gene expression analysis using real-time PCR. Methods [Internet]. 2010 Apr 1 [cited 2021 Dec 7]; 50(4):227–30. Available from: https://doi.org/10.1016/j.ymeth.2009.11.001

View Article Online
DOI: 10.1039/D5LC00052A

Interplay Between Dietary Fiber, Macrophages and Colonocytes in a Microfluidic Model of Host-Microbiota Interactions in Colorectal Cancer

Daniel Penarete-Acosta[1,†], Mohet Mittal[2,†], Sanjukta Chakraborty[3], Arum Han[1,2,4], Arul Jayaraman[1,2*]

[1] Department of Biomedical Engineering, Texas A&M University
[2] Artie McFerrin Department of Chemical Engineering, Texas A&M University
[3] Department of Medical Physiology, College of Medicine, Texas A&M University
[4] Department of Electrical and Computer Engineering, Texas A&M University
* Corresponding author. arulj@tamu.edu
† Equal contribution.

Data availability statement

The data supporting this article have been included as part of the Supplementary Information.